

## Effect of collectivity on the nuclear level density

Pratap Roy,\* K. Banerjee, M. Gohil, C. Bhattacharya, S. Kundu, T. K. Rana, T. K. Ghosh, G. Mukherjee, R. Pandey, H. Pai, V. Srivastava, J. K. Meena, S. R. Banerjee, S. Mukhopadhyay, D. Pandit, S. Pal, and S. Bhattacharya

*Variable Energy Cyclotron Centre, 1/AF, Bidhan Nagar, Kolkata 700 064, India*

(Received 22 May 2013; revised manuscript received 7 August 2013; published 16 September 2013)

Neutron evaporation spectra at backward angles from  $^{201}\text{Tl}^*$ ,  $^{185}\text{Re}^*$ , and  $^{169}\text{Tm}^*$  compound nuclei, having different ground-state deformations, have been measured at two excitation energies ( $E^* \sim 37$  and 26 MeV). The values of the inverse level density parameter ( $k$ ), extracted at these excitations using statistical model calculations, are observed to decrease substantially at the lower excitation energy ( $\sim 26$  MeV) for nuclei having large ground-state deformation (residues of  $^{185}\text{Re}^*$  and  $^{169}\text{Tm}^*$ ), whereas for near-spherical nuclei (residues of  $^{201}\text{Tl}^*$ ), the  $k$  value remains unchanged at the two energies. The decrease in  $k$  at the lower excitation energy for the deformed systems amounts to a relative increase in nuclear level density, indicating a collective enhancement. The present observation clearly establishes the existence of a strong correlation between collectivity and ground-state deformation.

DOI: [10.1103/PhysRevC.88.031601](https://doi.org/10.1103/PhysRevC.88.031601)

PACS number(s): 24.60.Dr, 21.10.Ma, 24.10.Pa, 25.70.Gh

Our understanding of the nuclear level density (NLD) function, which is an important ingredient in various theoretical models used for quantitative explanation of a number of physical phenomena in nuclear physics (yields of evaporation, fission, multifragmentation, spallation), astrophysics (thermonuclear reaction rates for nucleosynthesis), and technology (fusion-fission cross section for reactor design), is even today far from satisfactory. In recent years several studies have been carried out both theoretically and experimentally to understand the functional dependence of nuclear level density on key parameters, such as excitation energy [1], angular momentum [2–4], and isospin [5]. But one major issue which is yet to be resolved is the inter-relationship between collective excitations and nuclear level density as a function of excitation energy (or temperature). In nuclei, collective rotation and vibration involving several nucleons couple to the single-particle excitations. It has therefore been conjectured that any contribution of collective excitation would manifest itself as an enhancement in NLD. As the collective contributions appear due to both rotational as well as vibrational degrees of freedom, the effective nuclear level density at an excitation energy  $E^*$ , and angular momentum  $J$ , may be expressed as [6]

$$\rho(E^*, J) = \rho_{\text{int}}(E^*, J)K_{\text{coll}}(E^*), \quad (1)$$

where  $\rho_{\text{int}}(E^*, J)$  is the single-particle contribution to the total level density and  $K_{\text{coll}}(E^*) [=K_{\text{vib}}(E^*)K_{\text{rot}}(E^*)]$  is the collective enhancement factor. Here  $K_{\text{vib}}$  and  $K_{\text{rot}}$  are the vibrational and rotational contributions to the collective enhancement, respectively. For nuclei with appreciable ground-state deformation, the most significant contribution to the collective enhancement comes from the rotational excitations, whereas in the case of spherical nuclei, the collective enhancement is likely to be due to vibrational excitations.

The compound and daughter (evaporation residue) nuclei, which are deformed at ground state, are expected to be spherical at higher excitation energy due to the gradual

damping of long-range correlations, which are mainly responsible for the collective enhancement in NLD. Therefore the collective contribution in level density is also expected to die out at higher excitation, which is known as fadeout of collectivity. Björnholm *et al.* [7] have suggested a critical temperature  $T_c$ , beyond which the fadeout is expected.  $T_c$  is given by

$$T_c = \hbar\omega_0\beta_2 \sim 40A^{-1/3}\beta_2 \text{ MeV}, \quad (2)$$

where  $\omega_0$  is the mean oscillation frequency and  $\beta_2$  is the ground-state nuclear quadrupole deformation parameter.

Junghans *et al.* [8] made a quantitative estimate of  $K_{\text{rot}}(E^*)$  for an axially symmetric nuclei with quadrupole deformation  $|\beta_2| > 0.15$  and showed that  $K_{\text{rot}}(E^*)$  is directly related to the spin cutoff factor as given below:

$$K_{\text{rot}}(E^*) = \begin{cases} (\sigma^2 - 1)f(E^*) & \sigma^2 > 1 \\ 1 & \sigma^2 \leq 1. \end{cases} \quad (3)$$

Here,  $\sigma = \sqrt{\frac{IT}{\hbar^2}}$  is the spin cutoff factor,  $I = 2/5m_0AR^2(1 + \beta_2/3)$ , is the rigid body moment of inertia perpendicular to the symmetry axis,  $A$  is the mass number,  $R$  is the radius,  $T$  is the temperature of the nucleus, and  $m_0$  is the nucleon mass. The fadeout of  $K_{\text{rot}}(E^*)$  with excitation energy has been represented by the Fermi function  $f(E^*) = \{1 + \exp(\frac{E^* - E_{\text{cr}}}{d_{\text{cr}}})\}^{-1}$ , where the expressions for deformation-dependent critical energy  $E_{\text{cr}} (=120\beta_2^2 A^{1/3} \text{ MeV})$  and width  $d_{\text{cr}} (=1400\beta_2^2/A^{2/3} \text{ MeV})$  have been obtained from Ref. [9]. Typically,  $K_{\text{rot}}(E^*)$  rises sharply at low excitation energy to reach a near plateau (slowly increasing with energy) and then falls off (fadeout transition) at  $E \sim E_{\text{cr}}$  with a slope decided by  $d_{\text{cr}}$ .

On the experimental front, only a few attempts have been made in the recent past to look for the collective enhancement in nuclear level density and its subsequent fadeout at higher excitation energy. Junghans *et al.* [8] studied the yields of nuclei produced in the fragmentation of relativistic Pb and U projectiles. They observed that the yields of the projectile-like fragments near  $N = 126$  magic number did not comply with

\*pratap\_presi@yahoo.co.in

TABLE I. Details of the systems investigated and their different parameters.

System	$E_{\text{lab}}$ (MeV)	$E^*$ (MeV)	Major decay channel	Corresponding $ER$	$\beta_2$ value of the $ER$ [12]
${}^4\text{He} + {}^{165}\text{Ho}$	40	37.8	$3n$	${}^{166}\text{Tm}$	0.284
${}^4\text{He} + {}^{165}\text{Ho}$	28	26.1	$2n$	${}^{167}\text{Tm}$	0.283
${}^4\text{He} + {}^{181}\text{Ta}$	40	36.9	$3n$	${}^{182}\text{Re}$	0.240
${}^4\text{He} + {}^{181}\text{Ta}$	30	27.2	$2n$	${}^{183}\text{Re}$	0.230
${}^4\text{He} + {}^{197}\text{Au}$	40	37.7	$3n$	${}^{198}\text{Tl}$	-0.044
${}^4\text{He} + {}^{197}\text{Au}$	28	25.9	$2n$	${}^{199}\text{Tl}$	-0.044

the predicted stabilization against fission due to shell effect. Assuming that the neutralization of the shell effect was due to collective enhancement in level density (all these fragments were highly deformed in the ground state), they concluded that the fadeout of collectivity is independent of the ground-state deformation. On the other hand, Komarov *et al.* [10] attempted to extract information on collective enhancement and its fadeout by studying  $\alpha$ -particle evaporation from the  ${}^{178}\text{Hf}$  compound nucleus produced in a heavy-ion fusion reaction; however, they did not find any convincing evidence of the existence of collective enhancement and its fadeout in their data.

The nature of the controversy as well as the recent review of the underlying theoretical assumptions [11] warrants new measurements to independently verify the status of collective enhancement. Here we report a new experiment where we have measured neutron evaporation spectra from the populated  ${}^{169}\text{Tm}^*$ ,  ${}^{185}\text{Re}^*$ , and  ${}^{201}\text{Tl}^*$  compound nuclei having widely different ground-state deformations. Light-particle-induced reactions were chosen to keep the input angular momenta at low values ( $\sim 15\hbar$ ) and also to limit the number of effective decay channels. For these systems, the shell corrections are small enough that they do not affect the signature of collective enhancement. The experiment was done at two energies to observe the variation, if any, of the level density parameter with energy. In all the cases, the compound nuclei decayed predominantly by either  $2n$  or  $3n$  channels, leading to only one dominant daughter, which helped to extract the level density less ambiguously. Details of the nuclei investigated in this work have been described in Table I.

The present experiment was performed using  ${}^4\text{He}$  ion beam of energies  $E_{\text{lab}} = 40$  and 28 MeV (40 and 30 MeV for  ${}^{181}\text{Ta}$  target) from the cyclotron facility at Variable Energy Cyclotron Centre. Self-supporting foils of  ${}^{181}\text{Ta}$ ,  ${}^{165}\text{Ho}$  (thicknesses  $\sim 1$  mg/cm<sup>2</sup>), and  ${}^{197}\text{Au}$  (thickness  $\sim 500$   $\mu\text{g}/\text{cm}^2$ ) were used as targets. The compound nuclei  ${}^{201}\text{Tl}^*$  ( ${}^4\text{He} + {}^{197}\text{Au}$ ),  ${}^{185}\text{Re}^*$  ( ${}^4\text{He} + {}^{181}\text{Ta}$ ), and  ${}^{169}\text{Tm}^*$  ( ${}^4\text{He} + {}^{165}\text{Ho}$ ) were populated by the complete fusion reactions at the excitation energies,  $E^* \sim 37$  and 26 MeV. The emitted neutrons were detected using four liquid-scintillator (BC501A) detectors of dimension  $5'' \times 5''$  [13]. The neutron detectors were placed outside the scattering chamber at angles  $90^\circ$ ,  $105^\circ$ ,  $120^\circ$ , and  $150^\circ$  with respect to the beam direction at a distance of 150 cm from the target. To keep the background of the neutron detector at a minimum level, the beam dump was kept at 3 m away from the target and was well shielded with layers of lead and borated paraffin. The energy of the emitted neutrons has been

measured using the time-of-flight (TOF) technique whereas the neutron  $\gamma$  discrimination was achieved by both pulse shape discrimination (PSD) and TOF. In the present experiment, the start of the TOF was taken from a 50-element  $\text{BaF}_2$ -based low-energy  $\gamma$ -detector array [14]. The array was split into two blocks of 25 detectors each and were placed on the top and bottom of a thin wall reaction chamber (wall thickness  $\sim 3$  mm) in a staggered castle-type geometry.

The neutron kinetic energy spectra (Figs. 1, 2, and 3) were obtained from the corresponding TOF spectra, after subtracting the background. In converting the neutron TOF to neutron energy, the prompt  $\gamma$  peak in TOF spectrum was taken as the time reference. The efficiency correction for the neutron detectors were carried out using the Monte Carlo computer code NEFF [15]. The background and efficiency-corrected neutron energy spectra, measured at various laboratory angles, were transformed to the center-of-mass (c.m.) system using standard Jacobian transformation. The analysis of the experimental data was carried out using the statistical model code GEMINI++ [16]. The code employs the Monte Carlo technique to follow the complete decay chain of the initial compound nucleus through series of sequential decays of all intermediate products until they become unable to undergo further decay. The evaporation of light particles is calculated using Hauser-Feshbach formalism. The nuclear level density

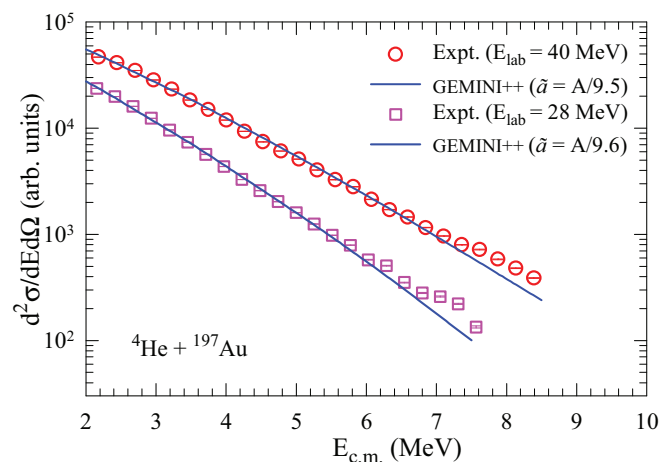


FIG. 1. (Color online) Measured neutron energy spectra (symbols) for the  ${}^4\text{He} + {}^{197}\text{Au}$  system at  $E_{\text{lab}} = 40$  and 28 MeV, along with statistical model calculation performed with GEMINI++ (continuous lines).

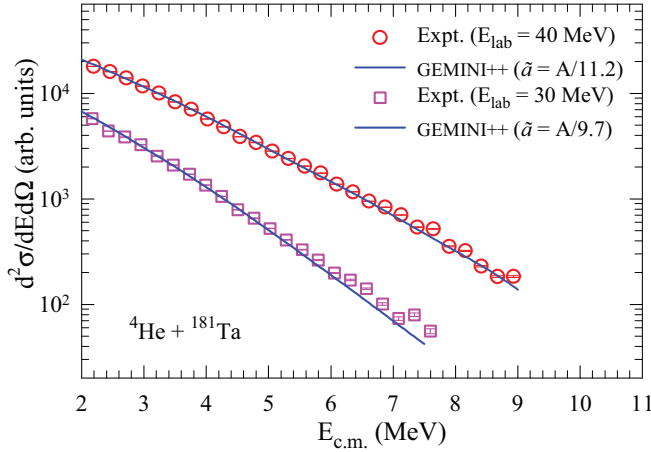


FIG. 2. (Color online) Same as in Fig. 1 for the  ${}^4\text{He} + {}^{181}\text{Ta}$  system at  $E_{\text{lab}} = 40$  and  $30$  MeV.

used in the present calculation is derived for a spherical nucleus in the independent-particle model with constant single-particle level density and is given by

$$\rho_{\text{int}}(E^*, J) = (2J + 1) \left[ \frac{\hbar^2}{2I} \right]^{\frac{3}{2}} \left[ \frac{\sqrt{a}}{12} \right] \frac{\exp(2\sqrt{aU})}{U^2}, \quad (4)$$

with

$$U = (E^* - E_{\text{rot}} + \delta P) \quad (5)$$

and  $E_{\text{rot}} = \frac{\hbar^2}{2I} J(J + 1)$ . Here,  $\delta P$  is the pairing correction, and  $a$  is the level density parameter. To take care of the distortion in the nuclear shape at large angular momenta due to the centrifugal forces, the rotational energy in Eq. [5] was replaced by the deformation-plus-rotational energy  $E_{\text{yrast}}(J)$  [16]. However, the present results were insensitive to the modification in the yrast energy as prescribed in Ref. [16]. In GEMINI++ the effect of shell structure in nuclear level density is taken care through the excitation-energy-dependent level

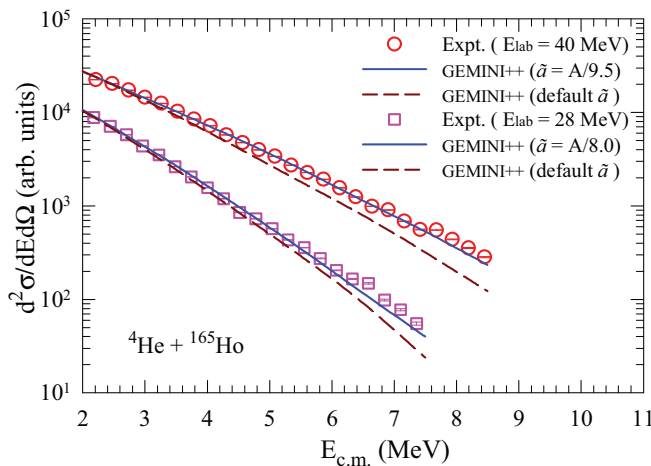


FIG. 3. (Color online) Same as in Fig. 1 for the  ${}^4\text{He} + {}^{165}\text{Ho}$  system at  $E_{\text{lab}} = 40$  and  $28$  MeV. Predictions of GEMINI++ with default level density parameter are shown by the dashed curves.

TABLE II. Fitted inverse level density parameter for different systems.

System	$U$ (MeV)	Fitted inverse level density parameter ( $k$ )	$T$ (MeV)	$T_c$ (MeV) [from Eq. (2)]
${}^4\text{He} + {}^{165}\text{Ho}$	35.7	$9.5 \pm 0.3$	1.37	2.06
${}^4\text{He} + {}^{165}\text{Ho}$	24.8	$8.0 \pm 0.5$	1.03	2.06
${}^4\text{He} + {}^{181}\text{Ta}$	35.1	$11.2 \pm 0.4$	1.40	1.62
${}^4\text{He} + {}^{181}\text{Ta}$	25.9	$9.7 \pm 0.5$	1.11	1.62
${}^4\text{He} + {}^{197}\text{Au}$	36.1	$9.5 \pm 0.6$	1.26	0.30
${}^4\text{He} + {}^{197}\text{Au}$	24.8	$9.6 \pm 0.7$	1.03	0.30

density parameter given by

$$a(U, J) = \tilde{a} \left[ 1 - h(U/\eta + J/J_\eta) \frac{\delta W}{U} \right], \quad (6)$$

where  $\delta W$  is the shell correction to the liquid drop mass and  $\tilde{a}$  is the level density parameter at higher excitation energy as expected from the liquid drop model. With  $h(x) = \tanh(x)$ , the prescribed values of  $\eta$  and  $\tilde{a}$  are 19 and  $A/7.3 \text{ MeV}^{-1}$  respectively. The transmission coefficients for the inverse absorption process have been calculated using real optical model potentials with the incoming wave boundary condition (IWBC) to ensure full absorption.

The shapes of the neutron energy spectra are mostly sensitive to the value of level density parameter. The value of the level density parameter usually estimated as  $\tilde{a} = A/k$ , where  $k$  is called the inverse level density parameter. The optimum values of  $k$  were extracted by fitting the experimental neutron spectra using the  $\chi^2$  minimization technique, which have been tabulated in Table II.

It is observed (see Table II) that the best-fit values of the inverse level density parameter decrease from  $9.5 \pm 0.3$  to  $8.0 \pm 0.5$  for the  ${}^4\text{He} + {}^{165}\text{Ho}$  system as the thermal excitation energy decreases from 35.7 to 24.8 MeV. Similar change (decrease) in  $k$  value from  $11.2 \pm 0.4$  to  $9.7 \pm 0.5$  has also been observed for the  ${}^4\text{He} + {}^{181}\text{Ta}$  system at the same excitation energy range. On the contrary, the  $k$  value remained almost same ( $9.5 \pm 0.6$  and  $9.6 \pm 0.7$ ) at both excitation energies in the case of the  ${}^4\text{He} + {}^{197}\text{Au}$  system. In other words, the above observation (the decrease of  $k$ ) suggests that there has been a relative enhancement in nuclear level density at lower excitation energy for the first two systems, whereas for the third system no such variation has been observed. The level density expression used in the present analysis [Eq. (4)] is based on the Fermi gas model, which is purely single particle in nature. Therefore the observed variation in  $k$  (or  $a$ ) may be a manifestation of the collective contributions to NLD, which is not accounted for in the calculations.

The nature of variation as seen above may be directly linked with the deformation of the respective systems. The ground-state deformations of the dominant daughter nuclei produced in the  ${}^4\text{He} + {}^{165}\text{Ho}$  ( $\beta_2 \sim 0.284$  for  ${}^{166,167}\text{Tm}$ ) and  ${}^4\text{He} + {}^{181}\text{Ta}$  ( $\beta_2 \sim 0.24$  for  ${}^{182,183}\text{Re}$ ) reactions are significantly higher than those produced in the  ${}^4\text{He} + {}^{197}\text{Au}$  reaction ( $\beta_2 \sim 0.044$  for  ${}^{198,199}\text{Tl}$ ). The collective enhancement factors calculated

using Eq. (3) for these systems indicate that there should be appreciable collective enhancement in the two deformed systems ( $K_{\text{coll}} \sim 80$ ) as compared to the nearly spherical third system ( $K_{\text{coll}} \sim 1$ ). So, the observed variation of inverse level density parameter with excitation energy for the deformed systems is clearly a signature of collectivity-induced modification (enhancement) of the level density, which is absent in case of nearly spherical system ( ${}^4\text{He} + {}^{197}\text{Au}$ ). This is further corroborated from the comparison of critical temperatures (see Table II); in deformed systems, the temperatures are well below the respective  $T_c$ , whereas it is reverse for the spherical system.

In an alternative prescription [16], an attempt has been made to incorporate the effect of collectivity in the standard Fermi gas description of NLD, by modifying  $\tilde{a}$  as given below:

$$\tilde{a} = \frac{A}{k_{\infty} - (k_{\infty} - k_0)\exp\left(-\frac{\kappa}{k_{\infty} - k_0} \frac{U}{A}\right)} \quad (7)$$

where  $\kappa(A) = 0.00517\exp(0.0345A)$  decides the nature of washout of long-range correlations. The default values of  $k_0$  and  $k_{\infty}$  are 7.3 and 12 MeV respectively. However, the above parametrization is insufficient to explain the observed variation of NLD in the present data (as shown in Fig. 3 by dashed curves for the  ${}^4\text{He} + {}^{165}\text{Ho}$  system), which further highlights the need to include explicit deformation dependence in  $\tilde{a}$  to explain the data.

In summary, the backward angle neutron evaporation energy spectra from  ${}^{201}\text{Tl}^*$ ,  ${}^{185}\text{Re}^*$ , and  ${}^{169}\text{Tm}^*$  compound nuclei have been measured at  $\sim 37$ - and 26-MeV excitation energies. The statistical model analysis of the experimental data have been carried out using GEMINI++ code to extract the

value of inverse level density parameter. It has been observed that for the deformed systems ( ${}^{185}\text{Re}^*$  and  ${}^{169}\text{Tm}^*$ ), there was significant reduction in the  $k$  value at lower excitation energy; however, no such variation of  $k$  was observed for the near-spherical  ${}^{201}\text{Tl}^*$  system. The decrease in  $k$  at lower excitation is suggestive of a relative increase in level density which may be a signature of collectivity. The observed variation of  $k$  in the present case cannot be explained by the excitation energy dependent formalism of  $k$  as given in Eq. (7). Though the absolute value of enhancement cannot be obtained from the present data in a model independent way, it has been found that the effect of collectivity (enhancement in the value of  $\tilde{a}$ ) is less at  $E^* \sim 36$  MeV than that at  $E^* \sim 28$  MeV.

Therefore it can be said that the present measurement clearly indicates the existence of collectivity induced modification of level density parameter, which is correlated with the ground state deformation of the system. The effect of collectivity is higher at lower excitation energy and decreases with increasing energy, which is manifested in the lowering of  $\tilde{a}$  at higher excitation energy. This is somewhat different from the trend as predicted in Ref. [8], in this excitation energy range ( $\sim 25$ – $35$  MeV). Further experimental investigation in wider excitation energy range together with the improvement of the statistical model codes to incorporate the deformation dependent collective enhancement factor directly in the calculation will be necessary to understand the effect of collectivity and its subsequent fadeout in more detail.

The authors are thankful to the VECC Cyclotron operators for smoothly running the accelerator during the experiment.

- 
- [1] S. Shlomo and J. B. Natowitz, *Phys. Lett. B* **252**, 187 (1990).  
 [2] K. Banerjee *et al.*, *Phys. Rev. C* **85**, 064310 (2012).  
 [3] P. Roy *et al.*, *Phys. Rev. C* **86**, 044622 (2012).  
 [4] Y. K. Gupta, B. John, D. C. Biswas, B. K. Nayak, A. Saxena, and R. K. Choudhury, *Phys. Rev. C* **78**, 054609 (2008).  
 [5] R. J. Charity and L. G. Sobotka, *Phys. Rev. C* **71**, 024310 (2005).  
 [6] A. V. Ignatyuk, K. K. Istekov, and G. N. Smirenkin, *Sov. J. Nucl. Phys.* **29**, 450 (1979).  
 [7] S. Björnholm, A. Bohr, and Mottelson, in *Proceedings of the International Conference on the Physics and Chemistry of Fission, Rochester, New York, 1973* (IAEA, Vienna, 1974), Vol. 1, p. 367.  
 [8] A. R. Junghans, M. de Jong, H. G. Clerc, A. V. Ignatyuk, G. A. Kulyaev, and K. H. Schmidt, *Nucl. Phys. A* **629**, 635 (1998).  
 [9] G. Hansen and A. S. Jensen, *Nucl. Phys. A* **406**, 236 (1983).  
 [10] S. Komarov, R. J. Charity, C. J. Chiara, W. Reviol, D. G. Sarantites, L. G. Sobotka, A. L. Caraley, M. P. Carpenter, and D. Seweryniak, *Phys. Rev. C* **75**, 064611 (2007).  
 [11] S. M. Grimes, *Phys. Rev. C* **78**, 057601 (2008).  
 [12] P. Möller, J. R. Nix, W. D. Myers, and W. J. Swiatecki, *At. Data Nucl. Data Tables* **59**, 185 (1995).  
 [13] K. Banerjee, T. K. Ghosh, S. Kundu, T. K. Rana, C. Bhattacharya, J. K. Meena, G. Mukherjee, P. Mali, D. Gupta, S. Mukhopadhyay *et al.*, *Nucl. Instrum. Methods Phys. Res., Sect. A* **608**, 440 (2009).  
 [14] D. Pandit, S. Mukhopadhyay, S. Bhattacharya, S. Pal, A. De, and S. R. Banerjee, *Nucl. Instrum. Methods Phys. Res., Sect. A* **624**, 148 (2010).  
 [15] G. Dietze and H. Klein, PTB-ND-22 Report, 1982 (unpublished).  
 [16] R. J. Charity, *Phys. Rev. C* **82**, 014610 (2010).